*Journal of Thermal Analysis and Calorimetry, Vol. 59 (2000) 847–858*

# MODELING OF THE DTG CURVES FOR OXIDATION OF A NANOSIZED MOLYBDENUM FERRITE COUPLING MECHANICS AND DIFFUSION

*V. Nivoix*[1], *P. Perriat*[2] *and B. Gillot*[3]*

[1]Université de Rouen, LASTSM, IUT, 76821 Mont Saint Aignan Cedex
[2]INSA de Lyon, GEMPPM-UMR CNRS 5510, 20, avenue Albert Einstein, 69621, Villeurbanne Cedex
[3]Laboratoire de Recherches sur la Réactivité des Solides, UMR CNRS 5613, 9, avenue Alain Savary, BP 47870-21078, Dijon Cedex, France

(Received November 26, 1998; in revised form March 16, 1999)

## Abstract

From a model for isothermal oxidation kinetics in nanosized ferrite spinels based on a diffusion-induced stress effect, the authors present a modeling of the DTG curves for the oxidation of $Fe^{2+}$ and $Mo^{3+}$ cations on octahedral sites of a molybdenum ferrite. This has been made by considering that the chemical diffusion coefficient is given by the relation $\tilde{D}=D_o \exp\left(-\frac{E'_a+pV_a}{RT}\right)$, when $D_o$ is a pre-exponential factor, $E'_a$ an activation energy and $V_a$ an activation energy induced by the oxidation.

**Keywords:** derivative thermogravimetry, diffusion-induced stress, modeling, molybdenum ferrite, oxidation kinetics

## Introduction

In previous publications [1, 2], the oxidation and reduction reactions in nanosized spinels with the formula $Fe_{3-x}M_xO_4$ where $0 \leq x \leq 1$ and M represents, in addition to iron, an oxidizable cation such $Cu^+$, $Mn^{2+}$, $Mo^{3+}$, $V^{3+}$, have been widely investigated by derivative thermogravimetry (DTG). We have shown that these nanosized powders with crystallite size below 100 nm exhibit a reactivity toward oxygen within the stability range of the spinel leading to the composition $Fe_{3-x}M_xO_{4+\delta}$ where δ denotes the oxidation degree. This reactivity is characterized by the appearance of a series of oxidation phenomena at relatively low temperature (<500°C) whose the oxidation temperature is governed by the activation energy for the ion jump. For example, the

* Author for correspondence. Tel.: + 33 80 39 61 42; Fax: + 33 80 39 61 67; e-mail: bgillot@satie.u-bourgogne.fr

*1418–2874/2000/ $ 5.00*

*Akadémiai Kiadó, Budapest*
*Kluwer Academic Publishers, Dordrecht*

octahedral B-site $Fe^{2+}$ ions are more mobile than the tetrahedral A-site $Fe^{2+}$ ions, so that they are oxidized near 200°C, while the A-sites are only oxidized above 350°C. Such a difference of reactivity is the evidence of a more covalent character of the tetrahedral Fe–O bonds [3].

A method of quantitative analysis based on the desummation of the DTG peaks of different oxidizable cations was developed to obtain a direct measure of the mixed distribution over both A and B-sites. However, the application of the desummation of the DTG peaks to quantitative low-temperature measurements of the distribution of cations in spinels is hampered by the fact that almost all peaks exhibit a tendency to overlap. Thereby, the peak areas calculated after desummation are not able to be accurately known and the desummation had to be confirmed by selective oxidation under isothermal conditions [4]. Another source of uncertainty is related to the fact that electron exchanges between cations occur above 400°C with no correlative change in the deviation from stoichiometry in the spinel [5].

Recently, we have described for isothermal oxidation of nanosized ferrites, a reaction mechanism based on a chemical and mechanical coupling model [6]. The model encounters the diffusion-induced stress effect generated in ferrite particles by chemical and lattice parameter gradients. In this contribution, emphasis is placed on the modeling of the DTG curves by taking into consideration a reaction mechanism coupling mechanics and diffusion. This has been made for the two first peaks of a molybdenum ferrite, $Fe_{2.47}Mo_{0.53}O_4$, when the proposed model from isothermal oxidations involved three parameters, the pre-exponential factor $D_o$, the thermal activation energy $E_a$ and the activation volume $V_a$.

## Experiments

The oxidation of the Fe and Mo cations has been studied in a nanoscaled molybdenum ferrite of the composition $Fe_{2.47}Mo_{0.53}O_4$. This material was prepared using the following chemistry route [7]: (i) precipitation of the mixed oxide, by adding a solution of $Fe^{2+}$, $Fe^{3+}$ and $Mo^{5+}$ chlorides to an alkaline medium, (ii) calcination of the precipitate up to 600°C, (iii) reduction under a $N_2$ (83.7%)–$H_2$ (7.3%)–$H_2O$ (9%) mixture at 600°C in order to obtain a ferrite with a spinel structure close to stoichiometry, (iv) quenching under the same $N_2$–$H_2$–$H_2O$ mixture. The shape of the powder grains determined from transmission electron microscopy (TEM) is spherical and the particles had a size of about 40 nm. The oxidations were performed in a static atmosphere of pure $O_2$ under isothermal or non isothermal (heating rate of 2°C $min^{-1}$) conditions in a Setaram TG 24 microbalance (symmetrical setup, resolution and noise level 0.1 μg) starting with 15 mg of powder.

Under non isothermal conditions, five peaks, corresponding to five distinct oxidation reactions may be revealed after desummation of the differential thermogravimetric curve (Fig. 1, curve a). Previous studies [4] allow to assign each peak to the oxidation of a specific cation: the oxidation of the octahedral and tetrahedral $Fe^{2+}$ ions is depicted by the peaks at 210 and 430°C, respectively, the peaks at 290 and 380°C are assigned to the oxidation of octahedral $Mo^{3+}$ and $Mo^{4+}$ ions, respectively, and fi-

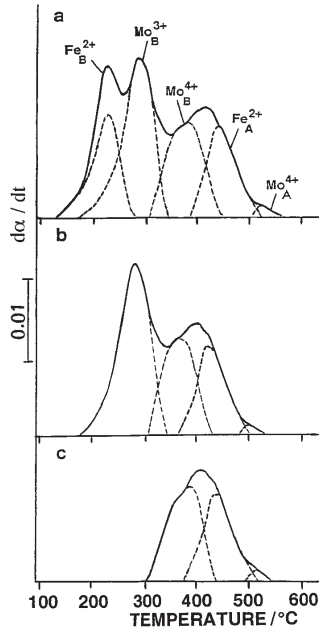


**Fig. 1** DTG curves $d\alpha/dt=f(T)$ and their desummation peaks for $Fe_{2.47}Mo_{0.53}O_4$ spinel. a – initial sample; b – oxidized sample at 165°C during 30 h showing the disappearance of the $Fe_B^{2+}$ ions peak; c – oxidized sample at 330°C for 24 h showing the disappearance of the $Fe_B^{2+}$ and $Mo_B^{3+}$ ions peaks

nally the last peak at about 500°C is assigned to the oxidation of tetrahedral $Mo^{4+}$ ions. However, as the peaks exhibit a tendency to overlap, the desummation has been confirmed by selective oxidation. Figure 1 (curve b) shows the profile of the peak attributed to $Mo_B^{3+}$ ions after selective oxidation under isothermal conditions (165°C for 30 h) of $Fe^{2+}$ ions of B-sites. Therefore, the ascending branch corresponding to the curve b represents only the oxidation of $Mo_B^{3+}$ ions. A similar experimental procedure was adopted for the oxidation of $Mo^{4+}$ ions on B-sites after elimination by oxidation of $Fe^{2+}$ and $Mo^{3+}$ ions for 24 h at 330°C (Fig. 1, curve c). Because the surface area of a given DTG peak is proportional to the quantity of the oxidized cation, by determining the surface area of each peak after desummation of the DTG curves, the quantity of each oxidizable cation may be calculated and a cation distribution proposed. For this composition, the cation distribution is given by the formula:

$$(Fe^{2+}_{0.58}Fe^{3+}_{0.40}Mo^{4+}_{0.02})_A(Mo^{3+}_{0.28}Mo^{4+}_{0.23}Fe^{2+}_{0.69}Fe^{3+}_{0.80})_B O^{2-}_4$$

## Isothermal oxidation and physical backgrounds

In addition to such straight-forward applications to the cation distribution of the derivative thermogravimetry, a more sophisticated use can be made of its analytical properties

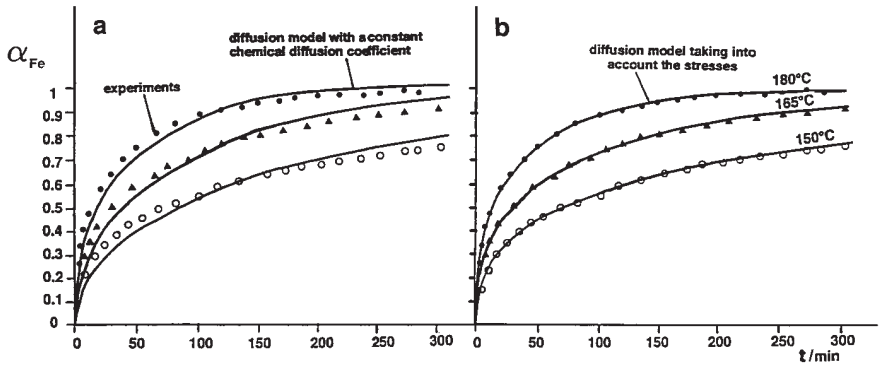


**Fig. 2** Evolution of the degree of reaction $\alpha_{Fe}$ with time for isothermal $Fe_B^{2+}$ oxidation under pure oxygen with a pressure of $4 \cdot 10^{-3}$ Pa. a – comparison of experimental data and a fit of these data obtained from a model based on a constant chemical diffusion coefficient; b – comparison of experimental data and a fit obtained by a diffusion model taking into account the effect of the stresses

exploiting the possibility of oxidizing the different cations independently under isothermal conditions. In order to determine the kinetics parameters, it has been established that the study of such isothermal oxidations at low temperature where the δ range of non stoichiometry is large, involves both thermodynamics and kinetics [8]. Thermodynamics gives the fraction of the Fe and Mo cations to be oxidized as a function of the temperature and the oxygen partial pressure while kinetics describes the process for such an oxidation. At relatively high oxygen partial pressure ($P_{O_2} > 10^3$ Pa), the degree of oxidation corresponds to the quasi-complete oxidation of the cations to their highest valence state, $Fe^{3+}$ for iron and $Mo^{6+}$ for molybdenum. As a consequence, transport within the grain which consists of the relaxation of the vacancies is the rate controlling. However, the classical model related to atomic diffusion via point defects described by the second Fick's law with a constant chemical diffusion coefficient is not able to explain completely the kinetics of oxidation.

The oxidation kinetics curves, $\alpha_i = f(t)$ determined as a function of temperature at a given high oxygen pressure ($i$=Fe, Mo) have a roughly parabolic shape, for both the oxidation of $Fe_B^{2+}$ and $Mo_B^{3+}$ ions as shown in Figs 2 and 3. The oxidation kinetics of $Mo_B^{3+}$ has been made after selective oxidation of $Fe_B^{2+}$ ions. The conversion degree, $\alpha_i$, is defined as $\alpha_{Fe}$ and $\alpha_{Mo} = \Delta m_{i(t)} / \Delta m_{i(\infty)}$ where $\Delta m_{i(t)}$ is the amount of $Fe_B^{2+}$ and $Mo_B^{3+}$ ions oxidized at B-sites at time $t$ and $\Delta m_{i(\infty)}$ is the corresponding amount after infinite time. In a case of isothermal oxidation, the chemical diffusion coefficient $\widetilde{D}$ can be classically written using the Arrhenius law :

$$\widetilde{D} = D_o \exp(-E_a / RT) \tag{1}$$

where $D_o$ is the preexponential factor and $E_a$ an activation energy. When the chemical diffusion coefficient is constant, the solution of Fick's second law, in the case of a spherical geometry is given by the equation [9]:

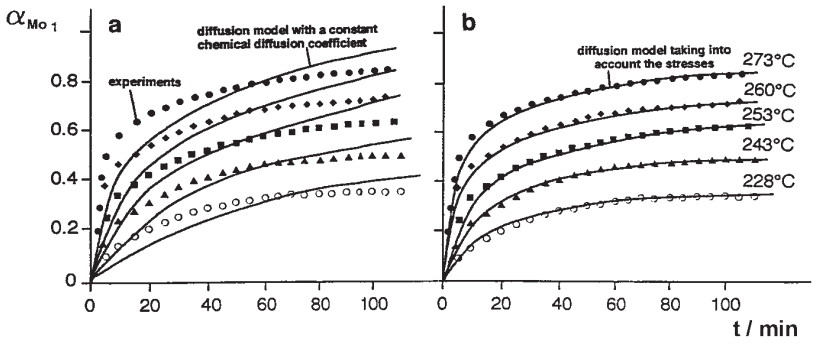


**Fig. 3** Evolution of the degree of reaction $\alpha_{Mo}$ with time for isothermal $Mo_B^{3+}$ oxidation under pure oxygen with a pressure of $4 \cdot 10^{-3}$ Pa. a – comparison of experimental data and a fit of these data obtained from a model based on a constant chemical diffusion coefficient; b – comparison of experimental data and a fit obtained by a diffusion model taking into account the effect of the stresses

$$\alpha_i = \frac{\bar{\delta}(t) - \bar{\delta}(t=0)}{\bar{\delta}(t=\infty) - \bar{\delta}(t=0)} = 1 - \frac{6}{\pi^2} \sum_{n=1}^{\infty} \frac{1}{n^2} \exp\left( -n^2 \frac{\pi^2}{r^2} \tilde{D} t \right) \quad (2)$$

where $\bar{\delta}(t)$ is the average value over the particle of the oxidation degree $\delta(r,t)$ and $r$ the radius of the particle. Note that $\bar{\delta}$, which is the quantity directly derived from the mass changes measured by TG, is characteristic of the material chemistry, while $\alpha_i$ is characteristic of the considered reaction kinetics between the initial state and the final state, respectively, defined by the homogeneous degree of oxidation $\delta(t=0)$ and $\delta(t=\infty)$. The experimental curves were tentatively fitted to Eq. (2). Figures 2a and 3a show the comparison between the experimental curves and that obtained by fitting. These figures reveal clearly that the two sets of curves are not in reasonable agreement. Compared with Fick's second law in the case of a constant chemical diffusion coefficient, the diffusion is faster at the beginning of the reaction before slowing down at the end. Thus, it is not possible to model the oxidation kinetics by considering a constant diffusion coefficient. We have to consider that the oxidation generates a composition gradient in the bulk of the grain and that within each particle, the deviation from stoichiometry, $\delta$, is higher on the surface than in the bulk. Consequently, the oxidized cations and the vacancies are located near the surface, while the low valency cations predominate in the bulk of the grain. Thus the lattice parameter has to vary continuously in the particle, leading to coherency stresses. Note that at the end of each reaction, when the cations in the particle are completely oxidized, the stresses must disappear. The effect of the stresses on diffusion kinetics has been described elsewhere from finite element calculation coupling mechanics and diffusion [6]. This will be discussed briefly next.

The chemical diffusion coefficient is written:

$$\tilde{D}=D_o \exp\left(-\frac{E'_a+pV_a}{RT}\right) \quad (3)$$

where $p$ is the isostatic local pressure, $V_a$ an activation volume and $E'_a$ a thermal activation energy. $V_a$ can be defined as the local volume change needed for a successful diffusion jump (Fig. 4). At low temperatures, the mechanical behavior of the material is purely elastic and a good approximation of the isostatic pressure can be obtained by the formula $p \approx E_\varepsilon$, where $E$ is the Young's modulus and $\varepsilon$ the deformation of the particle due to the gradient of oxidation degree. Under such conditions, $\tilde{D}$ is a function of the stress, i.e. when the material is subjected to compressive stresses ($p>0$), the diffusion slows down, while, when the material experiences tensile stresses ($p<0$), the diffusion becomes faster.

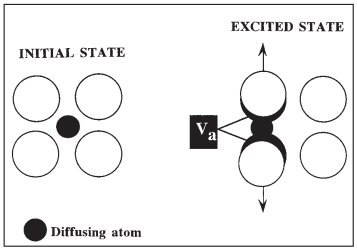


**Fig. 4** Scheme of a jump of diffusion and visualization of activation volume change during the diffusion of a cation via vacancies. It should be noted that the values obtained for the activation volume in ferrites are about 1.1 Ω/diffusing vacancy where Ω is the atomic volume of the diffusing cations

The isostatic pressure $p$ is obtained from the stress tensor $\sigma$:

$$p=-\frac{1}{3}Tr(\tilde{\sigma}) \quad (4)$$

after solving the equilibrium mechanical equation:

$$\mathrm{div}(\tilde{\sigma})=0 \quad (5)$$

under the additional condition of a deformation induced at each point by the diffusion deformation, $\tilde{\varepsilon}_{dif.}$ This deformation tensor is defined from the local lattice parameter, $a$, which depends on the local degree of oxidation $\delta(r,t)$:

$$\tilde{\varepsilon}_{dif}(r,t)=\frac{a(\tilde{\delta}(r,t))-a(\tilde{\delta}(t=0))}{a(\tilde{\delta}(t=0))}\tilde{1} \quad (6)$$

where $\tilde{1}$ is the unity tensor.

Table 1 gives for the two elementary oxidations, the values of the lattice parameter at the beginning, ($a(t=0)$) and the end ($a(t=\infty)$) of each reaction. The quantity, $a(t=\infty)-a(t=0)/a(t=0)$, is also given, since this latter is directly related to the magnitude of the stresses generated during the oxidation considered. The finite element method was used

after writing the problem with the framework of the classical variational method. The algorithm used for the modeling of the DTG curves is presented in Fig. 5.

**Table 1** Parameters relative to the two isothermal oxidation kinetics studied in a molybdenum ferrite

| Parameters | $Fe_B^{2+}$ oxidation | $Mo_B^{3+}$ oxidation |
|---|---|---|
| $a(t=0)$ (nm) | 0.8453 | 0.8416 |
| $a(t=\infty)$ (nm) | 0.8416 | 0.8359 |
| $\frac{a(t=\infty)-a(t=0)}{a(t=0)}$ | $-4.37\cdot10^{3}$ | $-6.77\cdot10^{3}$ |
| $D_o$ (nm$^2$ min$^{-1}$) | $5\cdot10^{11}$ | $2.2\cdot10^{22}$ |
| $E_a'$ (kJ mol$^{-1}$) | 100 | 246 |
| $V_a$ (cm$^3$ mol$^{-1}$) | 0.5 | 2 |

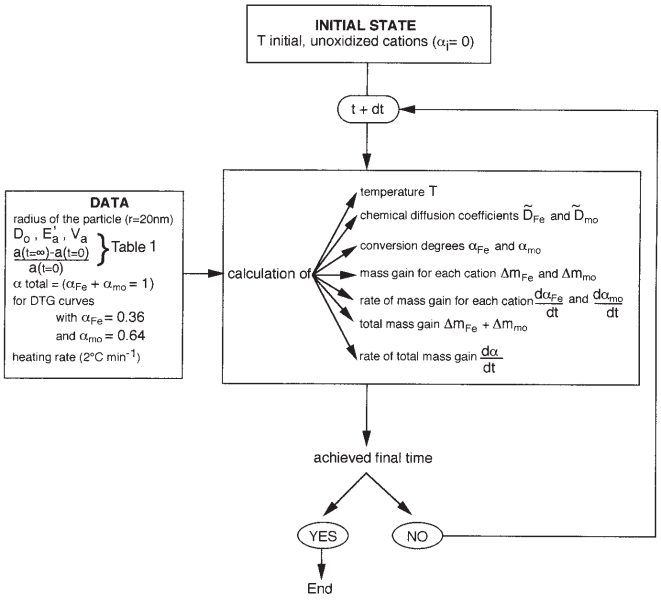


**Fig. 5** Algorithm used for the modeling of the DTG curves

The model coupling diffusion and mechanics was used to explain the experimental curves of Figs 2 and 3. We have, then, to find the set of parameters: $D_o$, $E_a'$ and $V_a$ (Table 1) which describes best the experimental curves. This has been done from the least-square fit when assuming a value of 1/3 for the Poisson coefficient. Figures 2b and 3b show the best fit between experiments and the model. Assuming that the Young's modulus in substituted ferrites is close to $10^6$ MPa [10, 11], the kinetics parameters relative to this fit are summarized in Table 1. The effect of stresses upon

diffusion which directly depends on the activation volume is more significant for the oxidation of the $Mo_B^{3+}$ cations than for that of $Fe_B^{2+}$ ones.

## Results and discussion

*Case of separated oxidations*

Earlier, the modeling was made on each oxidation in order to determine the influence of the activation volume and activation energy. From some studies concerning the oxidation in finely divided ferrites, it is found that the activation volume lies between 0 and 3 $cm^3\ mol^{-1}$ (a value of 2 $cm^3\ mol^{-1}$ induces atoms motion of 0.1 nm during a diffusion jump) and that the activation energy varies between 80 and 300 kJ $mol^{-1}$. In order to compare model with experiments (DTG curves), the oxidation rate $d\alpha/dt$ is plotted as a function of temperature. $\alpha$ is the global conversion degree, it is equal to 1 when all the cations ($Fe_B^{2+}$ and $Mo_B^{3+}$) are oxidized.

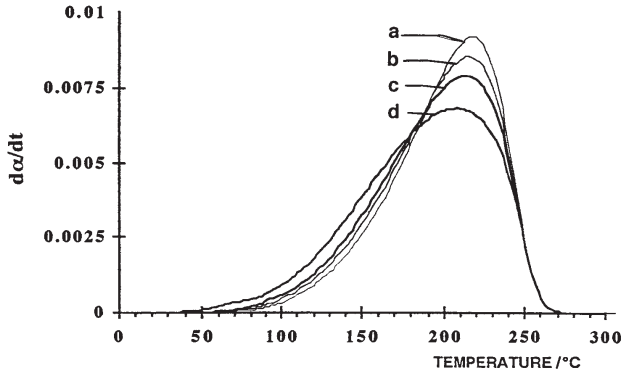


**Fig. 6** Influence of the activation volume on DTG curves for $Fe_B^{2+}$ oxidation. a – 0; b – 0.5; c – 1; d – 2 $cm^3\ mol^{-1}$

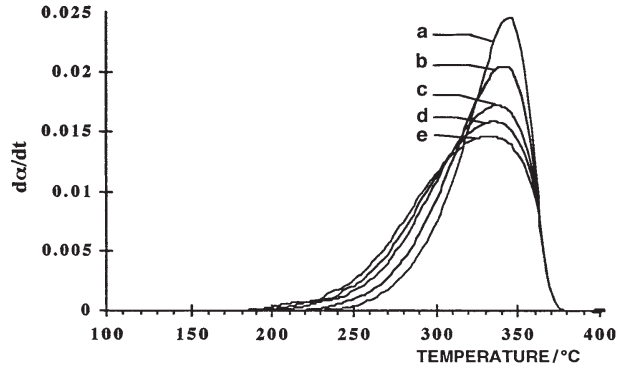


**Fig. 7** Influence of the activation volume on DTG curves for $Mo_B^{3+}$ oxidation. a – 0; b – 1; c – 2; d – 2.5; e – 3 $cm^3\ mol^{-1}$

In both cases of iron and molybdenum cations oxidation (Figs 6 and 7), the influence of the activation volume is identical when an increasing of the activation volume increases the reaction rate for the ascending branch while the curves overlap for the descending branch. Around the maxima, we observe a gradual decrease of the reaction rate as the activation volume increases. The interpretation for the observed differences in the DTG curves is explained assuming that at the beginning of the oxidation reaction, an increase of the activation volume facilitates the transfer of diffusing atoms at the surface of the grain which is subjected to tensile stresses. Then, for further oxidation, when the temperature increases, there are the cations in the bulk which are oxidized. Because the bulk is subjected to increasingly greater compressive stresses, the diffusion strongly decreases. At the end of the oxidation reaction when each oxidized cation and the vacancies predominate in the bulk of the grain, there are no gradient inside the particle. The chemical diffusion coefficient becomes constant that explain the overlapping of the DTG curves. Around the maxima, the decrease of the oxidation rate is more

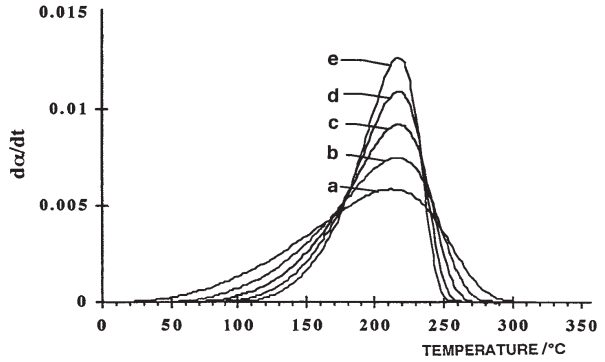


**Fig. 8** Influence of the activation energy on DTG curves for $Fe_B^{2+}$ ions oxidation. a – 60; b – 80; c – 100; d – 120; e – 140 kJ $mol^{-1}$

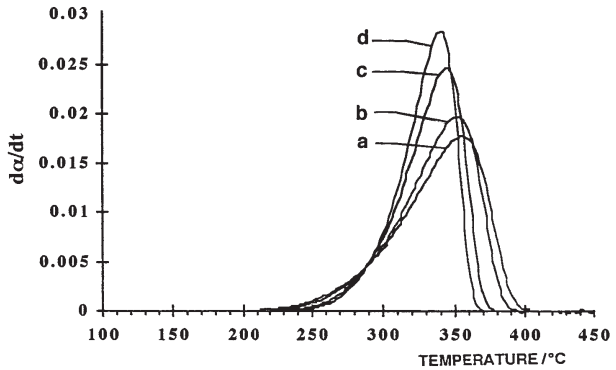


**Fig. 9** Influence of the activation energy on DTG curves for $Mo_B^{3+}$ ions oxidation. a – 60; b –200; c – 246; d – 280 kJ $mol^{-1}$

important for high values of $V_a$ because the expression (3) shows that increasing $V_a$ leads to a decrease of $\tilde{D}$.

The activation energy represents the necessary energy that allows for the diffusing atom to jump from initial to excited state. As shown in Figs 8 and 9, the curves exhibit virtually the same variation of $d\alpha/dt$ with $T$, a highest activation energy requiring a higher temperature for initiate the oxidation reaction. When the temperature gradually increases, the diffusion coefficient diminishes less quickly when $E_a$ increases and therefore the reaction is rapidly achieved. For the two oxidations, a high activation energy results in a sharper oxidation peak. It should be emphasized that in the case of $Mo_B^{3+}$ cations oxidation, the observed difference for the oxidation temperature range, in comparison to $Fe_B^{2+}$ cations oxidation originates in a higher activation energy and $D_o$ values for molybdenum cations.

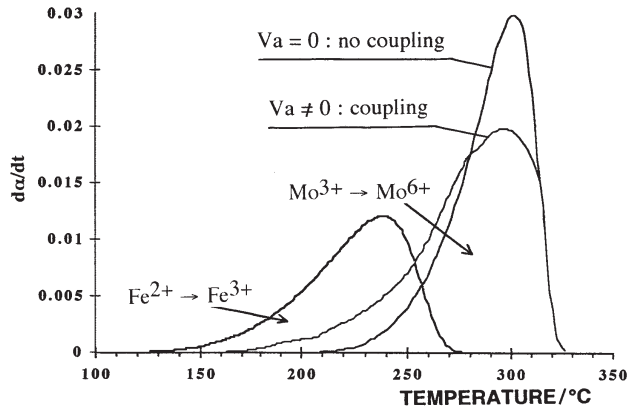


**Fig. 10** Influence of the coupling on the oxidation peak of $Mo_B^{3+}$ ions

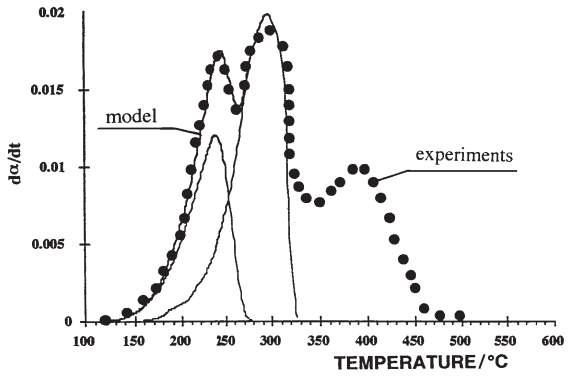


**Fig. 11** Modeling of the two first peaks and comparison with experimental curves

*Case of coupled reactions*

Due to the overlapping of the $Fe_B^{2+}$ and $Mo_B^{3+}$ peaks, when the $Mo_B^{3+}$ ions oxidize, the oxidation of $Fe_B^{2+}$ ions is already promoted. This imply that the first oxidation influence the second by the fact that the tensile stresses generated on the grain boundary during the oxidation of $Fe_B^{2+}$ ions activate the oxidation of $Mo_B^{3+}$ ions. By considering the expression of chemical diffusion coefficient for the two oxidations :

$$\widetilde{D}_{Fe} = D_{o_1} \exp\left( -\frac{E'_{a_1} + pV_{a_1}}{RT} \right) \text{ and } \widetilde{D}_{Mo} = D_{o_2} \exp\left( \frac{E'_{a2} + pV_{a2}}{RT} \right) \quad (7)$$

it can be seen that the isostatic pressure $p$ is associated to each oxidation and represents the coupling through the stress tensor. Figure 10 shows, as an example the influence of coupling on the $Mo_B^{3+}$ ions oxidation peak. The parameters $D_o$, $E'_a$ and $V_a$ to obtain the closest fit with the experimental curve are indicated in Table 2 and the Fig. 11 shows the modeling of the two first oxidation peaks. The values of $E_a$, $V_a$, $D_o$ are characteristic of each type of cation. The difference for the parameter values observed can be explained by considering the magnitude of the activation volume which depends on the order of magnitude of the stresses generated during the oxidation of each cation. The oxidation of a cation $M^{n+}$ to $M^{(n+m)+}$ involves concentration fluxes of $M^{(n+m)+}$ and vacancies, , from the surface to the bulk of the particle balanced by opposite concentration fluxes of $M^{n+}$ from the bulk to the surface. Two processes can contribute to the concentration fluxes of the cations: one involving cation motions, the other electron motions. Assuming that the vacancies are located in B-sites, the two elementary diffusion mechanism can be described by the following relations:

Oxidation of $Fe_B^{2+}$: $3Fe_B^{2+} \leftrightarrow 2Fe_B^{3+} +$

Oxidation of $Mo_B^{3+}$: $2Mo_B^{3+} \leftrightarrow Mo_B^{6+} +$

**Table 2** Parameters relative to the modeling of the DTG curves for the two first peaks oxidation in a molybdenum ferrite

| Cations | $D_o$/nm$^2$ min$^{-1}$ | $E_a$/kJ mol$^{-1}$ | $V_a$/cm$^3$ mol$^{-1}$ |
|---|---|---|---|
| $Fe_B^{2+}$ | $10^{16}$ | 145 | 0.5 |
| $Mo_B^{3+}$ | $10^{25}$ | 260 | 2 |

In the case of $Fe^{2+}$ ions oxidation a fraction of the concentration fluxes of the cations can be due to electron motions involved by charge exchanges between $Fe^{2+}$ and $Fe^{3+}$ ions present at equivalent crystallographic positions according to the Verwey's rule [12]. Such charge exchanges are not possible between $Mo^{3+}$ and $Mo^{6+}$ ions whose the difference of valency is greater than unity. In this case, the cation motions is only possible. This can explain a higher value for $V_a$ in the case of $Mo_B^{3+}$ cations, because $V_a$ is linked to the cations motion.

## Conclusions

A model has been proposed in order to explain the DTG curves for the oxidation in nanosized molybdenum ferrites. As temperature increases, stresses created during oxidation have a very strong influence on all following reactions. This implies that the chemical diffusion coefficient is not constant.

The model involves three parameters to express $\tilde{D}=D_o$, $E_a$ and $V_a$, which are characteristic of each cation, and which depend on the mechano-chemical coupling. It has to be noticed that such a model can be used only in case of nanosized ferrites, i.e. that the oxidation occurs by keeping the spinel lattice. In case of microsized spinels, a phase transformation occurs ($\gamma$-$Fe_2O_3 \rightarrow \alpha$-$Fe_2O_3$ type) during oxidation.

## References

1 B. Domenichini and B. Gillot, Solid State Ionics, 51 (1992) 7.
2 B. Gillot and A. Rousset, HCR Comprehensive Rev., 1 (1994) 69.
3 M. Laarj, I. Pignone, M. El Guendouzi, Ph. Tailhades and B. Gillot, Thermochim. Acta, 76 (1988) 355.
4 B. Gillot, J. Solid State Chem., 113 (1994) 163.
5 V. Nivoix, P. Perriat and B. Gillot, lonics, 2 (1996) 374.
6 P. Perriat, B. Domenichini and B. Gillot, J. Phys. Chem. Solids, 57 (1996) 1641.
7 L. Bouet, Ph. Tailhades, A. Rousset and B. Gillot, C. R. Acad. Sci., Paris, 312 série II (1991) 1507.
8 E. Kester and B. Gillot, J. Phys. Chem. Solids, 59 (1998) 1259.
9 B. Gillot, D. Delafosse and P. Barret, Mat. Res. Bull., 8 (1973) 1431.
10 Y. Adda and J. Philibert, La Diffusion dans les Solides, Institut National des Sciences et Techniques, Saclay, 2 (1996) p. 814.
11 B. B. Komalamba, K. Venkata Sivakumar and V. R. K. Murthy, J. Magn. Mater., 173 (1997) 59.
12 E. J. W. Verwey and P. W. Haaijman, Physica, 9 (1941) 979.